XIV International Conference on Topics in Astroparticle and Underground Physics (TAUP 2015) IOP Publishing
Journal of Physics: Conference Series **718** (2016) 052017 doi:10.1088/1742-6596/718/5/052017

Measurement of the Muon Content of Air Showers with IceTop

JG Gonzalez[1] for the IceCube Collaboration[2]

[1] University of Delaware
[2] http://icecube.wisc.edu/collaboration/authors/2015/07

Abstract. IceTop, the surface component of the IceCube detector, has measured the energy spectrum of cosmic ray primaries in the range between 1.6 PeV and 1.3 EeV. IceTop can also be used to measure the average density of GeV muons in the shower front at large radial distances (> 300 m) from the shower axis. Wel present the measurement of the muon lateral distribution function for primary cosmic rays with energies between 1.6 PeV and about 0.1 EeV, and compare it to proton and iron simulations. We also discuss how this information can be exploited in the reconstruction of single air shower events. By combining the information on the muon component with that of the electromagnetic component of the air shower, we expect to reduce systematic uncertainties in the inferred mass composition of cosmic rays arising from theoretical uncertainties in hadronic interaction models.

It is well known that the muon content of an air shower, together with a measure of its electromagnetic component, can be used to estimate the energy and mass of the primary [1] cosmic ray. The main issue with the use of the muon content as an estimate of primary mass is the possible systematic difference between simulated and real air showers, arising from the lack of knowledge of high energy hadronic interactions. An excess of muons has been reported by the HiRes-MIA and the Pierre Auger collaborations [2, 3]. Understanding the systematic difference in air shower muon content between simulations and data is one of the pressing issues in the physics of very high energy cosmic rays.

The IceTop detector is sensitive to the low-energy ($E \gtrsim 200$ MeV) muon component of air showers. We have previously presented estimates of the average muon Lateral Distribution Function (LDF) at lateral distances larger than 300 m—where the lateral distance of any point is defined as the closest distance from the point to the shower axis— and we showed how the measured muon density for vertical showers at a lateral distance of 600 m increases as a function of energy [4]. In this contribution we show an update of this analysis. The main improvements are the use of a semi-analytical model for the detector response (discussed in section 2), the inclusion of accidental coincidences and the comparison with CORSIKA [5] simulations using post-LHC models EPOS-LHC [6] and QGSJet-II-04 [7] in the last section.

1. General Features of IceTop

The IceCube detector consists of two major components. It can measure air showers on the surface with IceTop and high energy muon bundles with the in-ice detector, and both components in coincidence provided that the air shower axis goes through the in-ice detector. A detailed description of IceCube and IceTop has already been presented elsewhere [8]. The resulting cosmic ray energy spectrum measured with IceCube/IceTop can be found in these proceedings [9]. In

Content from this work may be used under the terms of the Creative Commons Attribution 3.0 licence. Any further distribution of this work must maintain attribution to the author(s) and the title of the work, journal citation and DOI.
Published under licence by IOP Publishing Ltd

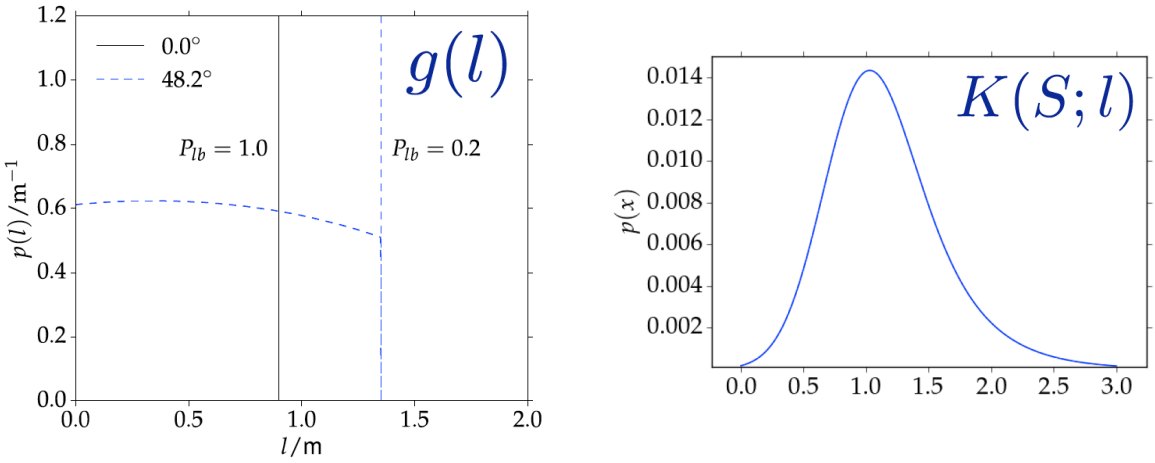

(a) Track length distribution.

(b) tank/PMT response kernel.

Figure 1: Semi-analytical model of detector response.

what follows, we will consider the specific characteristics of IceTop that are relevant for measuring the low-energy muon component of air showers.

IceTop is an air shower array consisting of 81 stations in a triangular grid with a separation of 125 m in its completed configuration. It is located above the deep IceCube detector at the geographical South Pole, covering an area of roughly one square kilometer. Each station consists of two ice Cherenkov tanks separated by ten meters. Each tank contains two Digital Optical Modules (DOMs) with a 10 inch photomultiplier tube (PMT) and electronics for signal processing and readout. A discriminator trigger occurs when the voltage in one of the DOMs in a tank has passed the discriminator threshold. The total charge collected at the PMT's anode, after digitization and baseline subtraction, constitutes the tank's signal.

The signal times are fitted with a function describing the shape of the shower front. The properties of the primary cosmic ray are reconstructed by fitting the measured signals with a Lateral Distribution Function (LDF) which includes an attenuation factor due to the snow cover on top of each tank. The primary energy is then given by the shower size S_{125}, defined as the signal at a lateral distance of 125 m.

2. A Model of Detector Response to Muons

Let us consider the response of an IceTop tank to an entering muon. The mean number of photoelectrons produced at the PMT when a single particle enters the tank is proportional to its track length. Muons cross the tank producing tracks that depend mostly on the geometrical configuration. For a uniform beam of muons entering a tank, the statistical distribution of track lengths $g(l)$ can be calculated analytically [10]. In the case of vertical muons, the distribution is a Dirac delta function since all muons traverse the tank from top to bottom. By definition, the signal recorded in this case is equal to one *Vertical Equivalent Muon* (VEM). For muons arriving forming an angle θ with the vertical, the distribution is a sum of two terms: a Dirac delta function centered at $1\,\mathrm{VEM}/\cos(\theta)$—produced by all muons that enter the tank through the top and exit through the bottom—and a continuous distribution that corresponds to muons that do not traverse the tank from top to bottom. The latter are what we call *corner clipping* muons. These two populations can be seen in Figure 1a. Given the track length of a muon, the signal probability distribution is given by an exponentially modified Gaussian kernel function $K(s|l)$, such as the one shown in Figure 1b [11]. This function takes care of effects such as the photon sampling and PMT collection efficiency. Figures 2a and 2b display the resulting signal

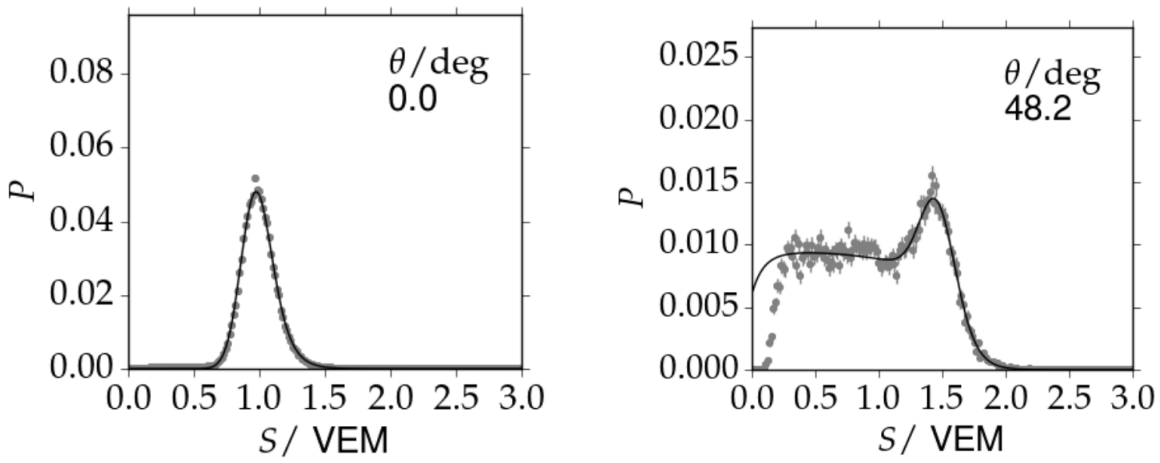

(a) 0° (b) 48°

Figure 2: Comparing the semi-analytical model with Geant4 simulations at two zenith angles.

distributions for two sets of parameters that differ only by their the zenith angle (0° and 48° respectively). The solid lines correspond to the signal distribution obtained using the Geant4 toolkit [12].

For an integer number of muons, the signal distribution is the multiple auto-convolution of the signal distribution of a single particle. The resulting distribution is multiplied with a Gaussian cumulative density function in the logarithm of the signal, which models the reduced efficiency for detecting low signals, caused by the discriminator trigger in each detector. All this can be summed in the following equations where $\langle N_\mu \rangle$ is the expectation value for the number of muons:

$$p\left(s \mid N_\mu = 1\right) = \int_0^{l_{max}} K(s \mid l, \mu, \sigma, \lambda)\, g(l \mid \theta)\, dl \tag{1}$$

$$p\left(s \mid N_\mu = n\right) = \int_0^{s} p\left(s \mid N_\mu = 1\right) p\left(s - t \mid N_\mu = n - 1\right) dt \tag{2}$$

$$p\left(s \mid \langle N_\mu \rangle\right) = \frac{1}{2}\left(1 + \mathrm{erf}\left(\frac{\log(s/s_{thr})}{\sigma_{thr}\sqrt{(2)}}\right)\right) \sum_{n=0}^{\infty} \frac{\langle N_\mu \rangle^n}{n!} e^{-\langle N_\mu \rangle} p\left(s \mid N_\mu = n\right) \tag{3}$$

The signal produced by all other particles is not modeled in detail. Most electrons and positrons loose their energy inside the tank. Their track lengths—and hence their signals—are typically smaller than those of muons, which causes a characteristic bi-modal signal distribution.

3. Muon Number Determination

We can see in Figure 3 how IceTop is sensitive to the number of muons in an air shower. Figure 3 is a 2D histogram of lateral distance and tank signal for air showers with fixed energy and zenith angle ($4\,\mathrm{PeV} < E < 5\,\mathrm{PeV}$ and $28° < \theta < 32°$ in this case). At large distances, there are two distinct populations. One population is the continuation of the main distribution which roughly follows a power law. The other population, with signals around 1 VEM, is made up mostly of tanks hit by one or more muons. These two populations are clearly seen in Figure 4, where we show the histograms of signals registered at selected fixed lateral distances.

The number of muons is determined by fitting the charge distributions at fixed energy, zenith, and lateral distance, as is illustrated in Figure 4, with the model described in section 2 using a

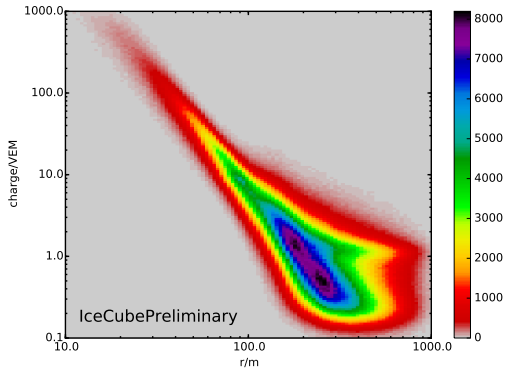

Figure 3: Signal distribution as a function of lateral distance for air showers with energies between 4 and 5 PeV, and zenith angle between 28° and 32°.

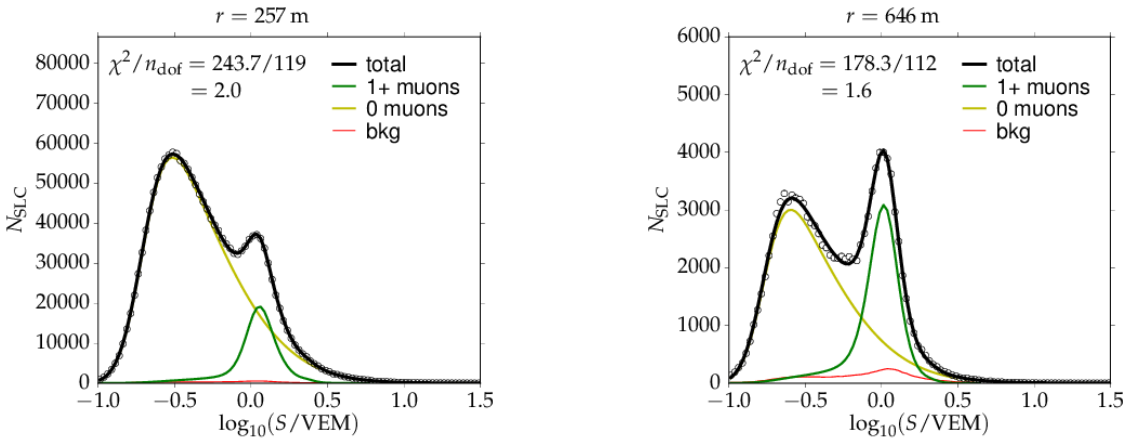

Figure 4: 1d histogram of signals at fixed lateral distance. The energy and zenith angle are the same as in Figure 3. The green line corresponds to the model summarized in equations 1 to 3. The yellow line corresponds to the EM particles. The red line is the contribution from accidental coincidences. Note how the relative contribution from muons is larger at the larger lateral distance

log-likelihood method. The fit includes three populations of signals. The signals with muons—the green line in Figure 4—are distributed according to the model described in Section 2. The signals with no muons—the yellow line–are distributed according to an empirically determined function of the form $p_{EM}(s) = As^b$. This expression is valid only when the mean expected signal from this component is much less than the threshold s_{thr}. The third population is made of signals that are not produced by the air shower but coincide in time with the event. The rate and distribution of these signals is determined directly from the data by selecting all signals in an off-time window 8 µs wide before the shower front arrives. The model has a total of 8 parameters: 3 in Equation 1, 3 in Equation 3 and 2 in $p_{EM}(s)$.

The result of the fit is the mean number of muons $\langle N_\mu \rangle$. The mean number of muons is divided by the cross-sectional area of the tanks to yield the muon density at that location. This assumes that the direction of motion of the muons coincides with the reconstructed air shower direction. According to simulations, this is correct within a degree.

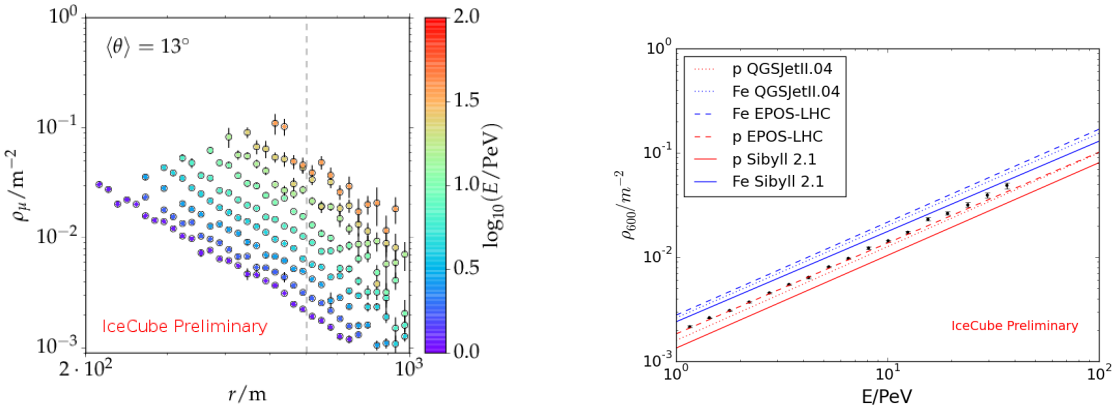

(a) (b)

Figure 5: Muon density as a function of lateral distance for quasi-vertical showers (∼13°) (left) and the interpolated value at 600 m from the shower axis compared to simulations using QGSJet-II-04 [7], EPOS-LHC[6] and Sibyll 2.1 [13] (right).

4. Results and Discussion

The results presented here were obtained with data collected between June 1st and June 30th 2011, but we expect to extend this dataset shortly. The resulting muon density as a function of lateral distance for quasi-vertical showers (∼13°) and some of the energies considered is shown in Figure 5a. This is interpolated to obtain ρ_{600}, the muon density at 600 m from the shower axis, which is shown in Figure 5b along with the average values of ρ_{600} obtained with CORSIKA simulations of hydrogen and iron primaries using various hadronic models.

The values of ρ_{600} for hydrogen and iron primaries bracket the measurements in all cases, although there are some interesting differences. The EPOS-LHC proton line is on top of the data, implying a lighter composition than what IceCube has inferred [9], while the QGSJet-II-04 lines imply a heavier composition. Note that the composition was inferred from IceCube data using the Sibyll 2.1 model [13]. It should be consistently derived using QGSJet-II-04 or EPOS-LHC to enable a fair comparison. It is prudent to remember that these are preliminary results. We are working to understand the systematic effects that can modify these results. These effects might not be negligible when compared to the differences between hadronic models.

References

[1] Kampert K-H and Unger M 2012 *Astropart.Phys.*, **35** 660–678
[2] Abu-Zayyad et al. 2000 *Phys. Rev. Lett.* **84** 4276–4279
[3] Aab A et al. 2014 *Phys.Rev.* **D91(3)** 032003
[4] Gonzalez JG et al. 2015 *EPJ Web Conf.* **99** 06002
[5] Heck D, Schatz G, Thouw T, Knapp J, and Capdevielle J N. 1998 CORSIKA: A Monte Carlo Code to Simulate Extensive Air Showers. *FZKA-6019*
[6] Pierog T, Karpenko Iu, Katzy J M, Yatsenko E, and Werner K 2015 *Phys. Rev.* **C92(3)** 034906
[7] Ostapchenko S 2013 *EPJ Web Conf.* **52** 02001
[8] Abbasi R et al 2013 *Nucl.Instrum.Meth.* **A700** 188–220
[9] Rawlins K et al 2015 Cosmic ray spectrum and composition from three years of IceTop and IceCube. In *these proceedings*
[10] Kégl B and Veberič D 2009 *Pierre Auger Observatory internal notes* (GAP-2009-043), arXiv:1502.03347
[11] Grushka E 1972 *Analytical Chemistry* **44(11)** 1733–1738
[12] Agostinelli S et al. 2003 *Nucl. Instrum. Meth.* **A506** 250–303 Allison A et al. 2006 *IEEE Trans. Nucl. Sci.* **53** 270–278
[13] Ahn EJ et al. 2009 *Phys.Rev.* **D80** 094003